Desalination and Water Treatment
www.deswater.com

47 (2012) 139–149
September

1944-3994/1944-3986 © 2012 Desalination Publications. All rights reserved
doi: 10.1080/19443994.2012.696796

Taylor & Francis
Taylor & Francis Group

Microwave heating-synthesized zeolite membrane for CO_2/CH_4 separation

Thiam Leng Chew[a,b,*], Abdul Latif Ahmad[a], Subhash Bhatia[a]

[a]*School of Chemical Engineering, Engineering Campus, Universiti Sains Malaysia, Seri Ampangan, 14300 Nibong Tebal, Pulau Pinang, Malaysia*
Tel. +604 5996490; Fax: +604 5941013; email: edvinchew_83@yahoo.com
[b]*Faculty of Engineering and Green Technology (FEGT), Perak Campus, Universiti Tunku Abdul Rahman, Jalan Universiti, Bandar Barat, 31900 Kampar, Perak, Malaysia*

Received 13 September 2011; Accepted 6 March 2012

ABSTRACT

H-SAPO-34 membrane was synthesized using microwave heating at 200°C for 2 h. Ba-SAPO-34 membrane was obtained by ion-exchanging the H-SAPO-34 membrane with Ba^{2+} cation. The separation of CO_2 from CO_2/CH_4 binary gas mixture was studied using design and analysis of experiments. The response surface methodology coupled with central composite design was used for modeling and analysis of the contribution of operating parameters (temperature, pressure difference across the membrane, CO_2 concentration in the feed) to the responses (CO_2 permeance and CO_2/CH_4 separation selectivity) during Ba-SAPO-34 membrane separation process. The process parameters were varied in the range of 30–180°C of temperature, 100–500 kPa of pressure difference and 5–50% of CO_2 concentration in the feed. The optimum condition for the process parameters was determined by setting the criteria so as to maximize the CO_2 permeance and CO_2/CH_4 separation selectivity. The optimum CO_2 permeance of 38.46×10^{-7} mol/m^2 s Pa and CO_2/CH_4 separation selectivity of 250.00 were determined at the temperature of 32.68°C, pressure difference of 101.19 kPa and 5.87% CO_2 concentration in the feed.

Keywords: Ba-SAPO-34; Membrane; Microwave; Carbon dioxide; Gas separation

1. Introduction

Gas separation is of vital environmental concern nowadays due to the issue of global climate change. The phenomenon of increasing greenhouse gas concentration, especially carbon dioxide (CO_2), in the atmosphere has drawn increasing interest among the researchers toward finding efficient methods for CO_2 capture before being emitted to atmosphere. This can be seen by numbers of articles published with the aim of finding potential gas separation process [1–3]. Separation of CO_2 is one such essential step in the natural gas processing plant. Conventional technologies used for CO_2 separation from gas mixtures are absorption using solvents, pressure swing adsorption and cryogenic distillation [3,4]. However, these methods bring about drawbacks such as complexity of the system, high energy consumption for solvent regeneration, flow problems caused by the viscosity of solvent and issue of equipment corrosion [5,6].

*Corresponding author.

Compared with the conventional gas separation technologies, membrane-based technologies are emerging as an alternative method for gas separation with higher energy efficiency, easier operating conditions and requirement of low capital costs due to no requirement to regenerate the absorbents [4,7–10]. There is increasing interest among researchers in focusing on gas separation studies using membranes [11–16]. Polymeric membranes are widely applied for gas separation in view of their characteristics such as low cost and ease of fabrication into desired gas separator modules [17–19]. However, their application for gas separation is limited due to the instability at high temperature and occurrence of plasticising effect in the presence of high CO_2 pressure, which results in reduced CO_2 separation performance of the polymeric membranes [19–22].

The deficiencies of polymeric membranes have prompted the development of zeolite membranes, which could overcome the problems for CO_2 gas separation. Zeolite membranes are the microporous inorganic membranes with higher thermal, mechanical and chemical stabilities compared to organic membranes [21]. Its uniform and molecular-sized pore structure with controlled host–sorbate interactions makes it attractive as a shape-selective material for gas separation [23,24]. Number of studies of gas permeation and separation using zeolite membranes such as MFI-type [25–30], FAU-type [20,31,32], A-type [33–36], DDR [37,38] and T-type [39,40] membranes is conducted. Silicoaluminophosphate (SAPO-34) membrane is one of the small-pore zeolite membranes which has been investigated extensively for gas permeation and separation [4,41–50]. Owing to the pore size of SAPO-34 zeolite, which is close to the kinetic diameter of CH_4 (0.38 nm) but larger than the kinetic diameter of CH_4 (0.33 nm), SAPO-34 zeolite membrane is therefore believed to be able to selectively separate CO_2 from CH_4.

MW heating offers number of advantages against conventional hydrothermal heating such as shorter synthesis time, rapid heating rate and production of small zeolite crystals with narrow size distribution [51–53]. Our group has been the first to report the synthesis of SAPO-34 zeolite membrane using MW heating to our best knowledge [54]. In our previous study, microwave (MW) heating was used to synthesis H^+-form SAPO-34 membrane. Ion exchange was then performed on the H^+ form of SAPO-34 membrane using different cations and followed by gas separation testing on the ion-exchanged SAPO-34 membranes [55]. The ion-exchanged SAPO-34 membranes exhibited enhanced separation performance in separating equimolar CO_2/CH_4 gas mixture. The Ba^{2+}-exchanged SAPO-34 (Ba-SAPO-34) membrane showed the highest performance in the separation studies of equimolar CO_2/CH_4 gas mixture, among all the ion-exchanged SAPO-34 membranes [55].

A statistical tool for determining the effect of significant process variable and the effect of the interaction between the variables on the process or product is known as design of experiments (DOE). Response surface methodology (RSM) coupled with central composite design (CCD), which is available in DOE statistical tool, is extensively adopted in order to determine the optimal settings of process parameters and to attain the process or product with desired quality in industries [56]. RSM has received considerable attention because it offers number of advantages: (1) reduction in the cost and number of experiments required, (2) more information per experiment compared to unplanned approaches, (3) better understanding of the process through determination of interaction between the process variables and (4) facilitation in the determination of the operating condition needed for the scale-up of the process [57]. RSM has been applied in different fields of studies by researchers and has been shown to be a powerful tool in optimizing the process or product [58–61].

In the present work, Ba-SAPO-34 zeolite membrane, which was prepared by MW heating followed by ion exchange with Ba^{2+} cation, was subjected to CO_2/CH_4 gas separation over 3 process variables: (1) temperature, (2) pressure difference and (3) CO_2 concentration (in terms of percentage) in the feed. The present study focuses on determining the optimum operating process condition for the optimization of CO_2 permeance and CO_2/CH_4 separation selectivity in the membrane-based gas separation process by applying DOE approach. The effect of the process variables toward CO_2/CH_4 separation performance of the Ba-SAPO-34 membrane was discussed.

2. Materials and methods

2.1. Preparation of Ba-SAPO-34 membrane

The Ba-SAPO-34 membrane was prepared in accordance with the procedures described by our previous work [55].

2.2. Characterization

Scanning electron microscopy, SEM (SUPRA 35VP-24-58) equipped with W-tungsten filament, was used to determine the morphology of Ba-SAPO-34 membrane. The XRD patterns of the Ba-SAPO-34 mem-

brane were obtained using high-resolution X-ray diffraction, XRD (Philips PANanalytical X-Pert PRO MRD PW3040, Spectris plc), with the source of Cu Ka ($k = 1.541874$ Å) and Kb ($k = 1.39225$ Å) monochromatic radiations.

2.3. CO_2/CH_4 gas separation studies

The Ba-SAPO-34 membrane, which was formed on a α-alumina disk support with thickness of 3 mm and diameter of 25 mm, was subjected to CO_2/CH_4 separation studies using a silicone gasket-sealed stainless steel module. Using two different mass flow controllers, CO_2 and CH_4 gas streams with different CO_2 concentrations (in terms of percentage) were fed to the membrane module. The membrane module was placed in an electronic-controlled oven so that the temperature for gas separation could be varied accordingly. The pressure of the feed side was controlled using a back pressure regulator while maintaining the pressure at the permeate side at atmospheric pressure in order to vary the pressure difference across the Ba-SAPO-34 membrane. The exit streams of permeate and retentate sides were analyzed using online gas chromatography (PERKIN ELMER, CLARUS 500) equipped with a thermal conductivity detector and a CARBOXEN-1010 column.

Permeance, P_i (mol/m^2 s Pa), of component gas i was calculated as follows:

$$P_i = \frac{J_i}{\Delta p_i} \tag{1}$$

where J_i is the flux of component i (mol/m^2 s) and Δp_i is the partial pressure difference of component i across the membrane (Pa)—the component i may refer to CO_2 or CH_4.

The CO_2/CH_4 separation selectivity of the membrane, $\alpha_{CO_2/CH4}$ was calculated from the ratio of the gas permeance:

$$\alpha_{CO_2/CH_4} = \frac{P_{CO_2}}{P_{CH_4}} \tag{2}$$

2.4. Design of experiments (DOE)

DOE was selected for the CO_2/CH_4 separation studies using Design Expert software version 6.0.6 (STAT-EASE Inc., Mineapolis, USA). In this statistical method, all variables were varied simultaneously in accordance with a set of experimental runs generated by Design Expert software. RSM coupled with CCD was used to optimize the process variables for the CO_2/CH_4 separation. RSM consists of mathematical techniques for modeling and analysis of problems where several variables influence a response of interest [62]. This method determines model equations using quantitative data from minimum number of experiments, followed by the analysis of variables or interaction between variables toward the responses and optimization of the responses [63].

Table 1 shows the independent variables with their ranges studied for CO_2/CH_4 separation in DOE studies. The independent variables in current CO_2/CH_4 separation study were temperature, pressure difference and CO_2 % in the feed with factor codes of A, B and C, respectively. The level of the independent variable was coded such that −1 represents low level and +1 represents high level. The CCD generally consists of a 2^n factorial, and it suggests $2n$ factorial runs, $2n$ axial runs and nc center runs, with n is number of variable [62]. The location of the axial points is at $(\pm\alpha, 0, 0)$, $(0, \pm\alpha, 0)$ and $(0, 0, \pm\alpha)$ where α represents the distance of the axial point from center and makes the design rotatable. The value of α was set to be 1 in current study.

A suitable approximation for the true functional relationship between response, y and the set of independent variables was determined using Design Expert software. A low-order polynomial as shown by Eq. (3) or (4) is usually employed for the approximation [59,62,64]:

First-order model:

$$y = \beta_0 + \beta_1 x_1 + \beta_2 x_2 + \ldots + \beta_n x_n + \varepsilon \tag{3}$$

Table 1
Ranges of independent variables studied for CO_2/CH_4 separation

Variable		Factor code	Level and range		
Name	Unit		−1	0	+1
Temperature	℃	A	30	105	180
Pressure difference	kPa	B	100	300	500
CO_2% in the feed	5–50	C	5.0	27.5	50.0

Second-order model:

$$y = \beta_0 + \sum_{i=1}^{n} \beta_i x_i + \sum_{i=1}^{n} \beta_{ii} x_i^2 + \sum \sum_{i<j} \beta_{ij} x_i X_j + \varepsilon \quad (4)$$

where y is the response, β_0, β_i, β_{ii}, and β_{ij} are the regression coefficients for intercept, linear, quadratic and interaction terms, respectively, x_i and x_j are the independent variables, x_i x_j is the first-order interaction between x_i and x_j, ε is the error and n is the number of independent variables. The responses studied in current work were CO_2 permeance and CO_2/CH_4 separation selectivity. Analysis of variance (ANOVA) was performed on the model, which predicts CO_2 permeance and CO_2/CH_4 separation selectivity, respectively, to establish its statistical significance. The responses were then optimized using numerical optimization approach available in Design Expert software.

3. Results and discussion

3.1. Full-factorial design

Table 2 shows the experiment design matrix with its corresponding responses for the CO_2/CH_4 gas separation studies. 2^3 full-factorial CCD design for three independent variables (*A*: temperature, *B*: pressure difference and *C*: CO_2% in the feed) was performed. Total 20 experiment runs were suggested by the CCD where it consisted of eight factorial points, six axial points and six replicates at the center points for the CO_2/CH_4 gas separation studies. The reproducibility of the data was checked by performing experimental runs of 15–20. The CO_2 permeance of $0.83–26.91 \times 10^{-7}$ mol/m^2 s Pa and the CO_2/CH_4 separation selectivity 23.58–276.43 were obtained. The low value of relative standard deviations, which were less than 5%, for the repeated run at the center point confirmed the reproducibility of both the responses.

Table 2
Experiment design matrix and responses for the separation studies of CO_2/CH_4

Run	Variable			Response	
	A Temperature, ℃	*B* Pressure difference, kPa	*C* CO_2% in the feed	CO_2 permeance, $\times 10^7$ mol/m^2 s Pa	CO_2/CH_4 separation selectivity
1	30	100	5	26.91	276.43
2	180	100	5	6.26	44.96
3	30	500	5	4.43	56.84
4	180	500	5	2.46	27.52
5	30	100	50	3.76	103.20
6	180	100	50	1.99	35.86
7	30	500	50	1.17	51.85
8	180	500	50	0.83	23.58
9	30	300	27.5	1.75	63.88
10	180	300	27.5	1.39	27.84
11	105	100	27.5	7.50	84.58
12	105	500	27.5	1.25	35.47
13	105	300	5	6.18	62.71
14	105	300	50	1.40	39.9
Repeated runs					
15	105	300	27.5	1.54	40.88
16	105	300	27.5	1.50	38.28
17	105	300	27.5	1.61	41.97
18	105	300	27.5	1.52	38.05
19	105	300	27.5	1.63	41.66
20	105	300	27.5	1.65	41.10
Mean				1.58	40.32
Standard deviation				0.06	1.57
Relative standard deviation, %				3.80	3.89

3.2. Response of CO_2 permeance

Table 3 shows the ANOVA for a 2^3 full-factorial CCD design of the CO_2 permeance. The quadratic model in term of the coded factor was chosen to describe the relationship between the response and the independent variables, as shown in Eq. (3). The positive sign (+) in front of the model terms indicates synergistic effect, while the negative sign (−) indicates antagonistic effect.

$$1/(\mathrm{CO_2\ Permenace}) = +0.61 + 0.10A + 0.24B + 0.26C + 0.075A^2 - 0.10B^2 - 0.13C^2 + 0.021AB + 0.035AC + 0.11BC \quad (5)$$

where A, B and C are the coded values of temperature, pressure difference and CO_2% in the feed, respectively.

The model F-value of 40.97 implied that the model was significant. CO_2% in the feed (C) affected the CO_2 permeance the most in view of its largest F-value of 151.55, compared to temperature (A) and pressure difference (B). In the current study, A, B, C, B^2, C^2, and BC were the model terms that were found to be significant at 95% confidence level for the model of $1/(CO_2$ permeance) because of their values of probability (Prob > F), which were less than 0.0500. Although the terms of AB and AC were not significant to the model due to their values of "Prob > F," which were greater than 0.1000, they were included in Eq. (3) to obtain a hierarchy model.

Fig. 1 shows the parity plot comparing the experimental $1/(CO_2$ permeance) and predicted $1/(CO_2$ permeance) obtained from Eq. (3). The value of correlation coefficient, R^2 of 0.9736, showed that there was an excellent agreement between experimental and predicted values of $1/(CO_2$ permeance). The suggested model for $1/(CO_2$ permeance) in Eq. (3) was shown to be accurate in predicting the $1/(CO_2$ permeance) over the ranges of temperature, pressure difference and CO_2% in the feed studied in the current study.

The three-dimensional response surface plots of the $1/(CO_2$ permeance) with its interaction between pressure difference and temperature, between CO_2% in the feed and pressure difference and between CO_2% in the feed and temperature are shown in Figs. 2–4. The $1/(CO_2$ permeance) increased with increase in temperature from 30 to 180˚C for pressure difference ranged 300–500 kPa with 27.5% CO_2 in the feed, as shown in Fig. 2. This trend was in agreement with the result reported by Li et al. [45]. When the separation temperature increased, the CO_2 diffusivity increased, but its surface coverage decreased. In this case, the decrease in surface coverage prevailed the increase in diffusivity with an increase in temperature. Hence, CO_2 permeance decreased, or in other words, the $1/(CO_2$ permeance) increased with an increase in temperature. It was observed in Fig. 3 that the $1/(CO_2$ permeance) increased, or in other words, the CO_2 permeance decreased with an increase in pressure difference for 5–50% CO_2 in the feed at 105˚C. This phenomenon was because of the fact that the increase in the gradient of adsorbed concentration was lower than the increase in CO_2 and CH_4 partial pressure

Table 3
Analysis of variance (ANOVA) for CO_2 permeance

Source	Sum of squares	Degree of freedom	Mean square	F-value	Prob > F
Model	1.58	9	0.18	40.97	< 0.0001
A	0.11	1	0.11	25.09	0.0005
B	0.57	1	0.57	133.33	< 0.0001
C	0.65	1	0.65	151.55	< 0.0001
A^2	0.015	1	0.015	3.56	0.0885
B^2	0.030	1	0.030	6.95	0.0249
C^2	0.048	1	0.048	11.29	0.0072
AB	3.687×10^{-3}	1	3.687×10^{-3}	0.86	0.3760
AC	0.010	1	0.010	2.34	0.1574
BC	0.092	1	0.092	21.31	0.0010
Residual	0.043	10	4.295×10^{-3}	–	–
Lack of fit	0.040	5	7.946×10^{-3}	12.33	0.0077
Pure error	3.222×10^{-3}	5	6.444×10^{-4}	–	–
Cor total	1.63	19	–	–	–

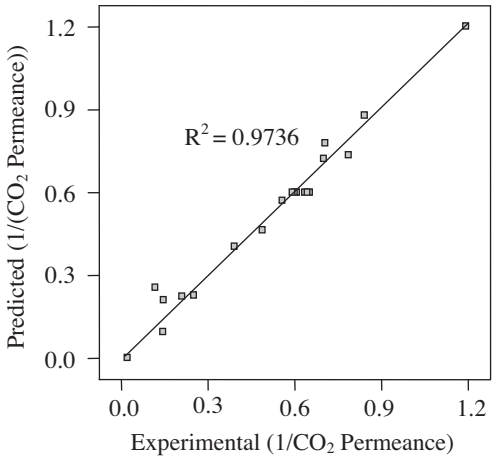

Fig. 1. Parity plot of experimental 1/(CO_2 permeance) and predicted 1/(CO_2 permeance) using Eq. (3).

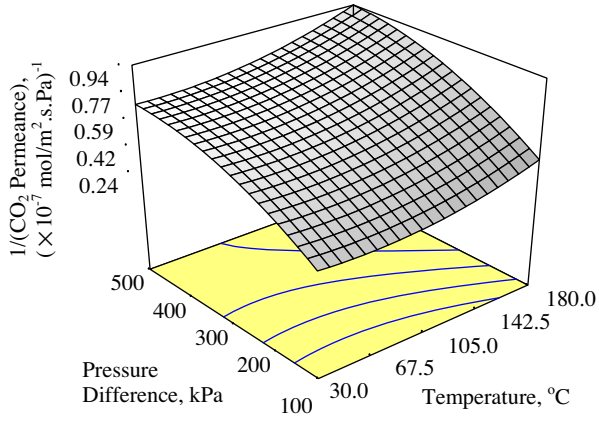

Fig. 2. Effect of pressure difference and temperature on 1/(CO_2 permeance) at 27.5% CO_2 in the feed.

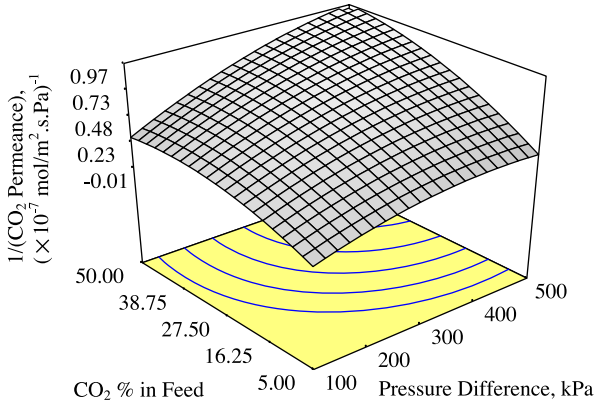

Fig. 3. Effect of pressure difference and CO_2% in the feed on 1/(CO_2 permeance) at the temperature of 105 °C.

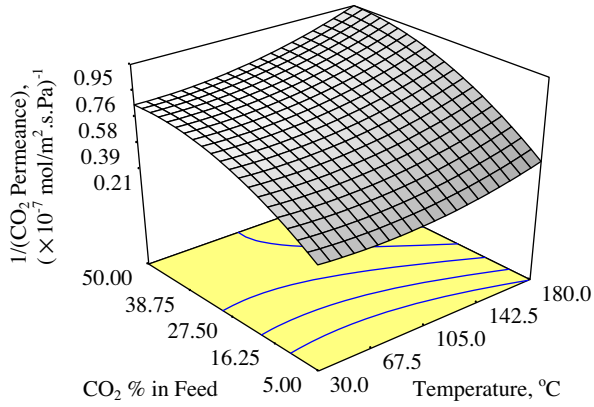

Fig. 4. Effect of temperature and CO_2% in the feed on 1/(CO_2 permeance) at a pressure difference of 300 kPa.

difference, respectively, across the membrane, when the pressure difference increased [28]. CO_2 permeance (gas flux divided by partial pressure difference) hence declined with an increase in pressure difference from 100 to 500 kPa. Figs. 3 and 4 show that the 1/(CO_2 permeance) increased with an increase in CO_2% in the feed from 5 to 50%.

3.3. Response of separation selectivity

Table 4 presents the ANOVA for 2^3 full CCD design of the CO_2/CH_4 separation selectivity. Eq. (4) was a quadratic model in terms of the coded factors generated to describe the relationship between the response and the independent variables. The positive sign (+) in front of the model terms indicates synergistic effect, while the negative sign (−) indicates antagonistic effect.

$$\begin{aligned}&1/(CO_2/CH_4 \text{ separation selectivity})\\&= +0.024 + 9.895\times10^{-3}A + 6.859\times10^{-3}B\\&\quad + 2.860\times10^{-3}C + 3.043\times10^{-3}A^2 - 2.736\\&\quad \times10^{-3}B^2 - 2.239\times10^{-3}C^2 + 6.307\times10^{-4}AB\\&\quad + 4.938\times10^{-4}AC - 4.940\times10^{-4}BC \qquad (6)\end{aligned}$$

where A, B and C are the coded value of temperatures, pressure difference and CO_2% in the feed, respectively.

The model F-value of 50.59 implied that the model was significant. It can be observed from Table 4 that the term F-value and hence the significance of variable's effect on CO_2/CH_4 separation selectivity decreased in the order of temperature (A) > pressure difference (B) > CO_2% in the feed (C). Values of "Prob > F" less than 0.0500 indicated that the model

Table 4
Analysis of variance (ANOVA) for CO_2/CH_4 separation selectivity

Source	Sum of squares	Degree of freedom	Mean square	*F*-value	Prob > *F*
Model	1.593×10^{-3}	9	1.770×10^{-4}	50.59	< 0.0001
A	9.792×10^{-4}	1	9.792×10^{-4}	279.92	< 0.0001
B	4.700×10^{-4}	1	4.700×10^{-4}	134.38	< 0.0001
C	8.178×10^{-5}	1	8.178×10^{-5}	23.38	0.0007
A^2	2.547×10^{-5}	1	2.547×10^{-5}	7.28	0.0224
B^2	2.058×10^{-5}	1	2.058×10^{-5}	5.88	0.0357
C^2	1.379×10^{-5}	1	1.379×10^{-5}	3.94	0.0752
AB	3.182×10^{-6}	1	3.182×10^{-6}	0.91	0.3627
AC	1.951×10^{-6}	1	1.951×10^{-6}	0.56	0.4724
BC	1.952×10^{-6}	1	1.952×10^{-6}	0.56	0.4722
Residual	3.498×10^{-5}	10	3.498×10^{-6}	–	–
Lack of fit	2.913×10^{-5}	5	5.826×10^{-6}	4.98	0.0514
Pure error	5.852×10^{-6}	5	1.170×10^{-6}	–	–
Cor total	1.628×10^{-3}	19	–	–	–

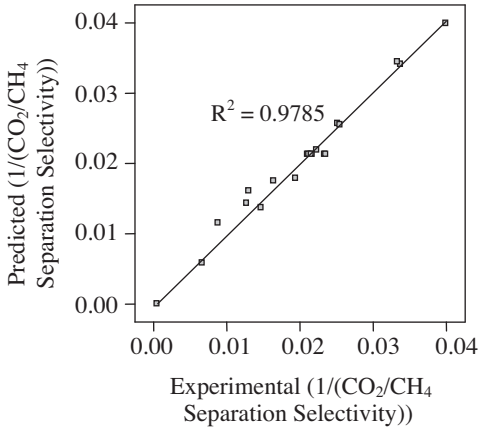

Fig. 5. Parity plot of experimental $1/(CO_2/CH_4$ separation selectivity) and predicted $1/(CO_2/CH_4$ separation selectivity) using Eq. (7).

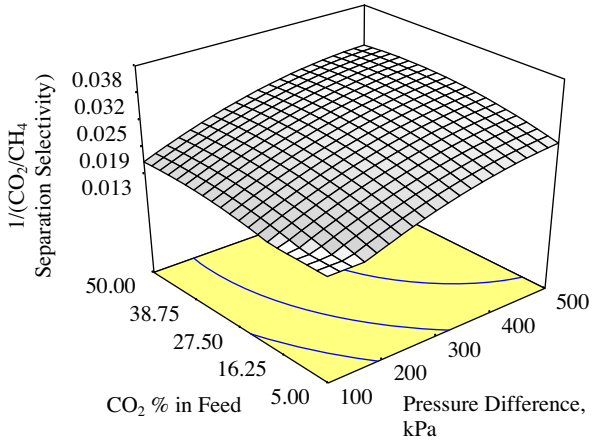

Fig. 7. Effect of pressure difference and CO_2% in the feed on $1/(CO_2/CH_4$ separation selectivity) at temperature of 105°C.

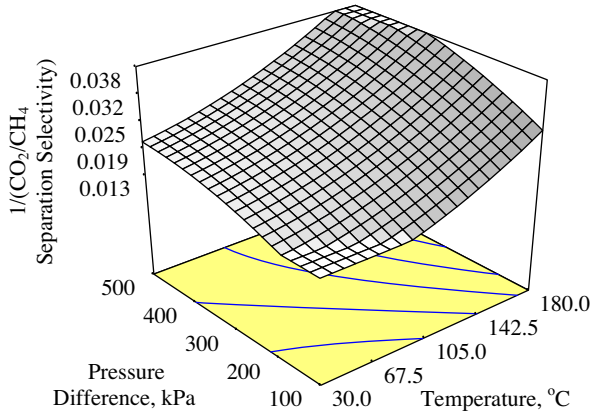

Fig. 6. Effect of pressure difference and temperature on $1/(CO_2/CH_4$ separation selectivity) at 27.5% CO_2 in the feed.

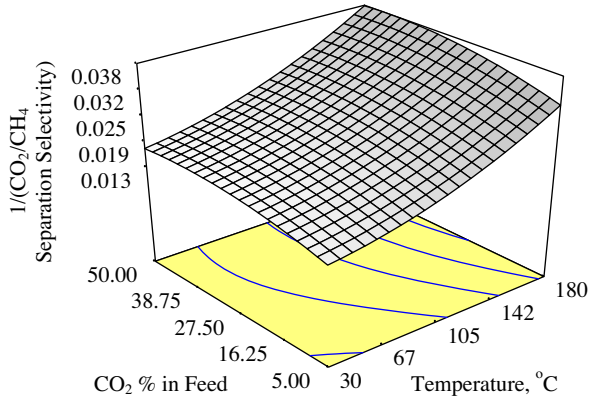

Fig. 8. Effect of temperature and CO_2% in the feed on $1/(CO_2/CH_4$ separation selectivity) at the pressure difference of 300 kPa.

terms were significant at 95% confidence level. *A*, *B*, *C*, A^2 and B^2 were found to be significant for the model of $1/(CO_2/CH_4$ separation selectivity) due to their values of "Prob > *F*," which were less than 0.0500. The insignificant terms of C^2, *AB*. *AC* and *BC* were included in Eq. (4) to obtain a hierarchy model.

For a model to be valid in predicting the response, there must be a good agreement between experimental and predicted responses. The values of $1/(CO_2/H_2$ separation selectivity) predicted using Eq. (4) was compared with the experimental values of $1/(CO_2/CH_4$ separation selectivity) as shown in Fig. 5. The value of correlation coefficient, R^2, obtained as 0.9785 showed that there was a good agreement between experimental and predicted responses. Hence, the suggested model for $1/(CO_2/CH_4$ separation selectivity) in Eq. (4) was accurate in predicting the $1/(CO_2/CH_4$ separation selectivity) over the ranges of temperature, pressure difference and CO_2% in the feed studied in the current study.

Figs. 6–8 show the three-dimensional response surface plots of the $1/(CO_2/CH_4$ separation selectivity) with its interaction between pressure difference and temperature, between CO_2% in the feed and pressure difference and between CO_2% in the feed and temperature. The $1/(CO_2/CH_4$ separation selectivity) increased with an increase in temperature from 30 to 180°C for 100–500 kPa pressure difference with 27.5% CO_2 in the feed. Increasing the temperature reduced the surface coverage of CO_2 on Ba-MW-2 membrane pore framework. The decline in CO_2 hindrance effect toward the permeation of CH_4 through the membrane pore framework resulted in the decrease in CO_2/CH_4 separation selectivity at a higher temperature [44]. As can be observed in Fig. 7, the $1/(CO_2/CH_4$ separation selectivity) increased, which meant that the CO_2/CH_4 separation selectivity decreased with an increase in pressure difference from 100 to 500 kPa for 5–50% CO_2 in the feed at 105°C. The increase in pressure difference influenced the CO_2 permeance more than the CH_4 permeance. Therefore, the CO_2 permeance decreased in a higher extent than the decline in CH_4 permeance, with increase in pressure difference from 100 to 500 kPa. For temperature that ranged from 30 to 180°C, the $1/(CO_2/CH_4$ separation selectivity) increased with an increase in CO_2% in the feed from 5 to 50% at 300 kPa, as shown in Fig. 8.

3.4. Optimization using RSM

Numerical optimization feature available in the Design Expert 6.06 software was used to determine the optimum condition. Design expert searched for a combination of factor levels that simultaneously satisfy the goal set for all the variables and responses. Table 5 shows the goal set in order to obtain the optimum condition for the responses. The goal was set to be within the high- and low-level ranges of the three independent variables: (A) temperature, (B) pressure difference and (C) CO_2% in the feed. The goal for the responses was to maximize both the CO_2 permeance and CO_2/CH_4 separation selectivity and hence to minimize both the $1(CO_2$ permeance) and $1/(CO_2/CH_4$ separation selectivity).

The solutions (optimum conditions) generated by the Design Expert with different total desirability were shown in Table 6. The solutions were sorted from the highest to the lowest value of desirability. The desirability function approach was used in the RSM for the optimization of operating conditions in the current work. Operating conditions that provide the "most desirable" response values were found using this approach. Each estimated response variable was transformed into an individual desirability value, d_i, using the desirability function [65]. The desirability value varies over the range $0 \leqslant d_i \leqslant 1$ where $(d_i = 0)$ represents a completely undesirable response value and $(d_i = 1)$ represents a completely ideal response value. The total desirability, *D* value, was obtained by combining the individual desirability. Solution 1 with the highest total desirability of 1.000 as shown in Table 6 was chosen for further process studies. At the optimum condition of solution 1, the $1/(CO_2$ permeance) value of $0.026(\times 10^{-7}$ mol/m^2 s Pa)$^{-1}$ and $1/(CO_2/CH_4$ separation selectivity) value of 0.004 were obtained, which were equivalent to CO_2 permeance of

Table 5
Goals for optimization of CO_2/CH_4 separation studies

Name		Goal	Lower limit	Upper limit
Variable	Temperature, °C	Within range	30	180
	Pressure difference, kPa	Within range	100	500
	CO_2% in the feed	Within range	5	50
Response	$1/(CO_2$ permeance), $(\times 10^7$ mol/m^2 s Pa)$^{-1}$	Minimum	0.037	1.205
	$1/(CO_2/CH_4$ separation selectivity)	Minimum	0.004	0.042

Table 6
Optimum condition for the 1/(CO_2 permeance) and 1/(CO_2/CH_4 separation selectivity)

Solution	Temperature, ℃	Pressure difference, kPa	CO_2% in the feed	1(CO_2 permeance), ($\times 10^7$ mol/ m^2 s Pa)$^{-1}$	1/(CO_2/CH_4 separation selectivity)	Total desirability
1	32.68	101.19	5.87	0.026	0.004	1.000
2	31.76	101.53	5.19	0.016	0.003	1.000
3	30.40	104.34	5.36	0.025	0.003	1.000
4	30.57	105.87	5.27	0.026	0.004	1.000
5	30.04	102.19	6.20	0.036	0.004	1.000
6	33.31	103.78	5.27	0.019	0.004	1.000
7	30.01	234.17	5.00	0.18	0.010	0.856
8	34.90	100.00	50.00	0.237	0.009	0.844
9	48.38	100.00	50.00	0.235	0.010	0.834
10	62.83	100.00	50.00	0.239	0.011	0.818

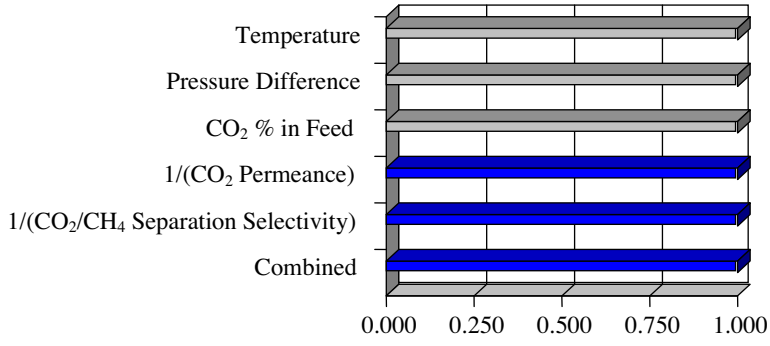

Fig. 9. Desirability of optimum conditions for solution 1.

38.46×10^{-7} mol/m^2 s Pa and CO_2/CH_4 separation selectivity of 250.00. Fig. 9 shows the individual and total desirability values of the variables and responses for solution 1.

In order to check the accuracy of the DOE, additional five experiments were conducted at the optimum operating condition generated by DOE. The generated optimum operating conditions were temperature of 32.68℃, pressure difference of 101.19 kPa and 5.87% CO_2 in the feed. Table 7 presents the separation result of the additional five experiments. By comparing the experimental values of CO_2 permeance and CO_2/CH_4 separation selectivity with the predicted values by the models, the mean error for CO_2

Table 7
Verification experiments at optimum operating conditions generated by DOE for the CO_2/CH_4 separation studies

Run	CO_2 permeance, $\times 10^7$ mol/m^2 s Pa		ΔError (%)	CO_2/CH_4 separation selectivity		ΔError (%)
	Experimental	Predicted (DOE)		Experimental	Predicted (DOE)	
1	35.55	38.46	7.57	244.06	250.00	2.38
2	36.49	38.46	5.12	235.45	250.00	5.82
3	37.85	38.46	1.59	248.61	250.00	0.56
4	36.30	38.46	5.62	235.45	250.00	5.82
5	36.67	38.46	4.65	239.68	250.00	4.13
Mean error			4.91			3.74

permeance and that for CO_2/CH_4 were both less than 5%, indicating good agreement between the experimental and predicted values. DOE with RSM was shown in current study to be an accurate tool in modeling and predicting the membrane performance for the CO_2/CH_4 separation process.

4. Conclusions

Ba-SAPO-34 zeolite membrane prepared in the current study exhibited good performance in separating CO_2 from CO_2/CH_4 gas mixtures. RSM coupled with CCD was successfully adopted to model the CO_2 permeance and CO_2/CH_4 separation selectivity as a function of temperature, pressure difference and CO_2% in the feed for the membrane. RSM in current study showed the significance of all the 3 independent variables and the effect of interaction between the independent variables on the responses. From the optimization of response using numerical optimization approach, optimum CO_2 permeance of 38.46×10^{-7} $mol/m^2 s Pa$ and CO_2/CH_4 separation selectivity of 250.00 were determined at the temperature of 32.68°C, pressure difference of 101.19 kPa and 5.87% CO_2 in the feed for Ba-SAPO-34 zeolite membrane in the current study. The values of optimum response predicted using the models were in good agreement with the actual value obtained experimentally.

Acknowledgements

The authors would like to acknowledge the financial support given by the Universiti Sains Malaysia (USM, Malaysia) in the form of Research University Grant (811043) and Fundamental Research Grant Scheme (6070021, 6071214) to support this project.

References

[1] H. Yang, Z. Xu, M. Fan, R. Gupta, R.B. Slimane, A.E. Bland, I. Wright, Progress in carbon dioxide separation and capture: A review, J. Environ. Sci. 20 (2008) 14–27.
[2] S. Adhikari, S. Fernando, Hydrogen membrane separation techniques, Ind. Eng. Chem. Res. 45 (2006) 875–881.
[3] G.Q. Lu, J.C. Diniz da Costa, M. Duke, S. Giessler, R. Socolow, R.H. Williams, T. Kreutz, Inorganic membranes for hydrogen production and purification: A critical review and perspective, J. Colloid Interface Sci. 314 (2007) 589–603.
[4] S. Li, C.Q. Fan, High-flux SAPO-34 membrane for CO_2/N_2 separation, Ind. Eng. Chem. Res. 49 (2010) 4399–4404.
[5] M.L. Gray, Y. Soong, K.J. Champagne, H. Pennline, J.P. Baltrus, R.W. Stevens, Jr, R. Khatri, S.S.C. Chuang, T. Filburn, Improved immobilized carbon dioxide capture sorbents, Fuel Process. Technol. 86 (2005) 1449–1455.
[6] F. Zheng, D.N. Tran, B.J. Busche, G.E. Fryxell, R.S. Addleman, T.S. Zemanian, C.L. Aardahl, Ethylenediamine-modified SBA-15 as regenerable CO_2 sorbent, Ind. Eng. Chem. Res. 44 (2005) 3099–3105.
[7] M. Freemantle, Membranes for gas separation: Advanced organic and inorganic materials being developed for separations offer cost benefits for environmental and energy-related processes, Chem. Eng. News 83 (2005) 49–57.
[8] E.J. Granite, T. O'Brien, Review of novel methods for carbon dioxide separation from flue and fuel gases, Fuel Process. Technol. 86 (2005) 1423–1434.
[9] J.W. Phair, S.P.S. Badwal, Materials for separation membranes in hydrogen and oxygen production and future power generation, Sci. Technol. Adv. Mater. 7 (2006) 792–805.
[10] A.F. Ismail, P.S. Goh, S.M. Sanip, M. Aziz, Transport and separation properties of carbon nanotube-mixed matrix membrane, Sep. Purif. Technol. 70 (2009) 12–26.
[11] M. Mohammadi Demochali, A.A. Ghoreyshi, G. Najafpour, Development of a multicomponent mass transport model for predicting CO_2 separation behavior from its mixture with natural gas and hydrogen using zeolite membranes, Desalin. Water Treat. 34 (2011) 190–196.
[12] M. Miyamoto, A. Takayama, S. Uemiya, K. Yogo, Gas permeation properties of amine loaded mesoporous silica membranes for CO_2 separation, Desalin. Water Treat. 34 (2011) 266–271.
[13] P. Sysel, E. Minko, M. Hauf, K. Friess, V. Hynek, O. Vopicka, K. Pilnacek, M. Sipek, Mixed matrix membranes based on hyperbranched polyimide and mesoporous silica for gas separation, Desalin. Water Treat. 34 (2011) 211–215.
[14] M. Nomura, K. Momma, Y. Negishi, E. Matsuyama, S. Kimura, Preparation of silica hybrid membranes for high temperature gas separation, Desalin. Water Treat. 17 (2010) 288–293.
[15] B. Zornoza, P. Gorgojo, C. Casado, C. Téllez, J. Coronas, Mixed matrix membranes for gas separation with special nanoporous fillers, Desalin. Water Treat. 27 (2011) 42–47.
[16] O.C. David, D. Gorri, I. Ortiz, A.M. Urtiaga, Dual-sorption model for H_2/CO_2 permeation in glassy polymeric Matrimid membrane, Desalin. Water Treat. 27 (2011) 31–36.
[17] H. Lin, B.D. Freeman, Gas permeation and diffusion in cross-linked poly(ethylene glycol diacrylate), Macromolecules 39 (2006) 3568–3580.
[18] H. Lin, E. Van Wagner, B.D. Freeman, L.G. Toy, R.P. Gupta, Plasticization-enhanced hydrogen purification using polymeric membranes, Science 311 (2006) 639–642.
[19] S. Basu, A.L. Khan, A. Cano-Odena, C. Liu, I.F.J. Vankelecom, Membrane-based technologies for biogas separations, Chem. Soc. Reviews 39 (2010) 750–768.
[20] K. Weh, M. Noack, I. Sieber, J. Caro, Permeation of single gases and gas mixtures through faujasite-type molecular sieve membranes, Micro. Meso. Mater. 54 (2002) 27–36.
[21] W.J. Koros, R. Mahajan, Pushing the limits on possibilities for large scale gas separation: Which strategies? J. Membr. Sci. 175 (2000) 181–196.
[22] S.P. Kaldis, G.C. Kapantaidakis, G.P. Sakellaropoulos, Polymer membrane conditioning and design for enhanced CO_2–N_2 separation, in: J.A. Pajares, J.M.D. Tascón (eds.), Coal Science and Technology, Elsevier, Amsterdam, 1995, pp. 1927–1930.
[23] D. Shekhawat, D.R. Luebke, H.W. Pennline, A review of carbon dioxide selective membranes, A Topical Report United State Department of Energy, 2003. Available from: http://www.osti.gov/bridge/servlets/purl/819990-vf3LSt/native/819990.pdf.
[24] Y. Li, J. Liu, W. Yang, Formation mechanism of microwave synthesized LTA zeolite membranes, J. Membr. Sci. 281 (2006) 646–657.
[25] D.W. Shin, S.H. Hyun, C.H. Cho, M.H. Han, Synthesis and CO_2/N_2 gas permeation characteristics of ZSM-5 zeolite membranes, Micro. Meso. Mater. 85 (2005) 313–323.
[26] V. Sebastián, I. Kumakiri, R. Bredesen, M. Menéndez, Zeolite membrane for CO_2 removal: Operating at high pressure, J. Membr. Sci. 292 (2007) 92–97.

[27] G.T.P. Mabande, M. Noack, A. Avhale, P. Kölsch, G. Georgi, W. Schwieger, J. Caro, Permeation properties of bi-layered Al-ZSM-5/Silicalite-1 membranes, Micro. Meso. Mater. 98 (2007) 55–61.
[28] M.P. Bernal, J. Coronas, M. Menéndez, J. Santamaría, Separation of CO_2/N_2 mixtures using MFI-type zeolite membranes, AIChE J. 50 (2004) 127–135.
[29] E. Piera, C.A.M. Brenninkmeijer, J. Santamaría, J. Coronas, Separation of traces of CO from air using MFI-type zeolite membranes, J. Membr. Sci. 201 (2002) 229–232.
[30] J.C. Poshusta, R.D. Noble, J.L. Falconer, Temperature and pressure effects on CO_2 and CH_4 permeation through MFI zeolite membranes, J. Membr. Sci. 160 (1999) 115–125.
[31] X. Gu, J. Dong, T.M. Nenoff, Synthesis of defect-free FAU-type zeolite membranes and separation for dry and moist CO_2/N_2 mixtures, Ind. Eng. Chem. Res. 44 (2005) 937–944.
[32] K. Sato, K. Sugimoto, Y. Sekine, M. Takada, M. Matsukata, T. Nakane, Application of FAU-type zeolite membranes to vapor/gas separation under high pressure and high temperature up to 5 MPa and 180˚C, Micro. Meso. Mater. 101 (2007) 312–318.
[33] N. Nishiyama, M. Yamaguchi, T. Katayama, Y. Hirota, M. Miyamoto, Y. Egashira, K. Ueyama, K. Nakanishi, T. Ohta, A. Mizusawa, T. Satoh, Hydrogen-permeable membranes composed of zeolite nano-blocks, J. Membr. Sci. 306 (2007) 349–354.
[34] Y. Li, H. Chen, J. Liu, W. Yang, Microwave synthesis of LTA zeolite membranes without seeding, J. Membr. Sci. 277 (2006) 230–239.
[35] N. Das, D. Kundu, M. Chatterjee, The effect of intermediate layer on synthesis and gas permeation properties of NaA zeolite membrane, J. Coat. Technol. Res. 7 (2010) 383–390.
[36] X. Xu, W. Yang, J. Liu, L. Lin, N. Stroh, H. Brunner, Synthesis of NaA zeolite membrane on a ceramic hollow fiber, J. Membr. Sci. 229 (2004) 81–85.
[37] S. Himeno, T. Tomita, K. Suzuki, K. Nakayama, K. Yajima, S. Yoshida, Synthesis and permeation properties of a DDR-type zeolite membrane for separation of CO_2/CH_4 gaseous mixtures, Ind. Eng. Chem. Res. 46 (2007) 6989–6997.
[38] T. Tomita, K. Nakayama, H. Sakai, Gas separation characteristics of DDR type zeolite membrane, Micro. Meso. Mater. 68 (2004) 71–75.
[39] S.M. Mirfendereski, T. Mazaheri, M. Sadrzadeh, T. Mohammadi, CO_2 and CH_4 permeation through T-type zeolite membranes: Effect of synthesis parameters and feed pressure, Sep. Purif. Technol. 61 (2008) 317–323.
[40] Y. Cui, H. Kita, K.-I. Okamoto, Preparation and gas separation performance of zeolite T membrane, J. Mater. Chem. 14 (2004) 924–932.
[41] M. Hong, S. Li, H.F. Funke, J.L. Falconer, R.D. Noble, Ion-exchanged SAPO-34 membranes for light gas separations, Micro. Meso. Mater. 106 (2007) 140–146.
[42] M. Hong, S. Li, J.L. Falconer, R.D. Noble, Hydrogen purification using a SAPO-34 membrane, J. Membr. Sci. 307 (2008) 277–283.
[43] S. Li, G. Alvarado, R.D. Noble, J.L. Falconer, Effects of impurities on CO_2/CH_4 separations through SAPO-34 membranes, J. Membr. Sci. 251 (2005) 59–66.
[44] S. Li, J.G. Martinek, J.L. Falconer, R.D. Noble, T.Q. Gardner, High-pressure CO_2/CH_4 separation using SAPO-34 membranes, Ind. Eng. Chem. Res. 44 (2005) 3220–3228.
[45] S. Li, J.L. Falconer, R.D. Noble, SAPO-34 membranes for CO_2/CH_4 separations: Effect of Si/Al ratio, Micro. Meso. Mater. 110 (2008) 310–317.
[46] S. Li, M.A. Carreon, Y. Zhang, H.H. Funke, R.D. Noble, J.L. Falconer, Scale-up of SAPO-34 membranes for CO_2/CH_4 separation, J. Membr. Sci. 352 (2010) 7–13.
[47] J.C. Poshusta, V.A. Tuan, E.A. Pape, R.D. Noble, J.L. Falconer, Separation of light gas mixtures using SAPO-34 membranes, AIChE J. 46 (2000) 779–789.
[48] Y. Tian, L. Fan, Z. Wang, S. Qiu, G. Zhu, Synthesis of a SAPO-34 membrane on macroporous supports for high permeance separation of a CO_2/CH_4 mixture, J. Mater. Chem. 19 (2009) 7698–7703.
[49] Z. Lixiong, J. Mengdong, M. Enze, S.-K.I. Hakze Chon, U. Young Sun, Synthesis of SAPO-34/ceramic composite membranes, Stud. Surf. Sci. Catal. 105 (1997) 2211–2216.
[50] M.A. Carreon, S. Li, J.L. Falconer, R.D. Noble, SAPO-34 seeds and membranes prepared using multiple structure directing agents, Adv. Mater. 20 (2008) 729–732.
[51] J. Motuzas, A. Julbe, R.D. Noble, A. van der Lee, Z.J. Beresnevicius, Rapid synthesis of oriented silicalite-1 membranes by microwave-assisted hydrothermal treatment, Micro. Meso. Mater. 92 (2006) 259–269.
[52] Y. Li, W. Yang, Microwave synthesis of zeolite membranes: A review, J. Membr. Sci. 316 (2008) 3–17.
[53] G. Zhu, Y. Li, H. Zhou, J. Liu, W. Yang, FAU-type zeolite membranes synthesized by microwave assisted *in situ* crystallization, Mater. Lett. 62 (2008) 4357–4359.
[54] T. Chew, A. Ahmad, S. Bhatia, Rapid synthesis of thin SAPO-34 membranes using microwave heating, J. Porous Mater. 18 (2011) 355–360.
[55] T.L. Chew, A.L. Ahmad, S. Bhatia, Ba-SAPO-34 membrane synthesized from microwave heating and its performance for CO_2/CH_4 gas separation, Chem. Eng. J. 171 (2011) 1053–1059.
[56] L.-I. Tong, Y.-C. Chang, S.-H. Lin, Determining the optimal re-sampling strategy for a classification model with imbalanced data using design of experiments and response surface methodologies, Expert Syst. Appl. 38 (2011) 4222–4227.
[57] G. Vicente, M. Martínez, J. Aracil, Optimisation of integrated biodiesel production. Part I. A study of the biodiesel purity and yield, Biores. Technol. 98 (2007) 1724–1733.
[58] M.-S. Fan, A.Z. Abdullah, S. Bhatia, Hydrogen production from carbon dioxide reforming of methane over Ni-Co/MgO-ZrO_2 catalyst: Process optimization, Int. J. Hydrogen Energy 36 (2011) 4875–4886.
[59] Y. Sun, W. Xu, W. Zhang, Q. Hu, X. Zeng, Optimizing the extraction of phenolic antioxidants from kudingcha made frrom Ilex kudingcha C.J. Tseng by using response surface methodology, Sep. Purif. Technol. 78 (2011) 311–320.
[60] K.L. Low, S.H. Tan, S.H.S. Zein, D.S. McPhail, A.R. Boccaccini, Optimization of the mechanical properties of calcium phosphate/multi-walled carbon nanotubes/bovine serum albumin composites using response surface methodology, Mater. Design 32 (2011) 3312–3319.
[61] L. Switzar, M. Giera, H. Lingeman, H. Irth, W.M.A. Niessen, Protein digestion optimization for characterization of drug-protein adducts using response surface modeling, J. Chromatogr. A 1218 (2011) 1715–1723.
[62] D.C. Montgomery, Design and Analysis of Experiments. Wiley, Hoboken, NJ, (2009).
[63] Y.F. Yeong, A.Z. Abdullah, A.L. Ahmad, S. Bhatia, Process optimization studies of p-xylene separation from binary xylene mixture over silicalite-1 membrane using response surface methodology, J. Membr. Sci. 341 (2009) 96–108.
[64] S.L. Wee, C.T. Tye, S. Bhatia, Process optimization studies for the dehydration of alcohol-water system by inorganic membrane based pervaporation separation using design of experiments (DOE), Sep. Purif. Technol. 71 (2010) 192–199.
[65] G. Derringer, R. Suich, Simultaneous optimization of several response variables, J Quality Technol. 12 (1980) 214–219.